

# We are IntechOpen, the world's leading publisher of Open Access books Built by scientists, for scientists

6,900

Open access books available

185,000

International authors and editors

200M

Downloads

Our authors are among the

154

Countries delivered to

TOP 1%

most cited scientists

12.2%

Contributors from top 500 universities



WEB OF SCIENCE™

Selection of our books indexed in the Book Citation Index  
in Web of Science™ Core Collection (BKCI)

Interested in publishing with us?  
Contact [book.department@intechopen.com](mailto:book.department@intechopen.com)

Numbers displayed above are based on latest data collected.  
For more information visit [www.intechopen.com](http://www.intechopen.com)



# Ferroelectric Domain Imaging Multiferroic Films Using Piezoresponse Force Microscopy

Hongyang Zhao, Hideo Kimura, Qiwen Yao,  
Lei Guo, Zhenxiang Cheng and Xiaolin Wang

Additional information is available at the end of the chapter

<http://dx.doi.org/10.5772/52519>

## 1. Introduction

Recently, multiferroic materials with the magnetoelectric coupling of ferroelectric (or anti-ferroelectric) properties and ferromagnetic (or antiferromagnetic) properties have attracted a lot of attention.[1-4] Among them,  $\text{BiFeO}_3$ (BFO) and  $\text{YMnO}_3$  has been intensively studied. For such  $\text{ABO}_3$  perovskite structured ferroelectric materials, they usually show antiferromagnetic order because the same B site magnetic element except  $\text{BiMnO}_3$  is ferromagnet. While for the  $\text{A}_2\text{BB}'\text{O}_6$  double perovskite oxides, the combination between B and B' give rise to a ferromagnetic coupling. They are also expected to be multiferroic materials. Several bis-muth-based double perovskite oxides ( $\text{BiBB}'\text{O}_6$ ) have aroused great interest like  $\text{Bi}_2\text{NiMnO}_6$ ,  $\text{La}_2\text{NiMnO}_6$ ,  $\text{BiFeO}_3\text{-BiCrO}_3$ . But as we know, few researches are focused on  $\text{Bi}_2\text{FeMnO}_6$ . We believe it is particular interesting to investigate  $\text{Bi}_2\text{FeMnO}_6$  (BFM). The origin of the ferromagnetism in these compounds has been discussed in many reports. According to Goodenough-Kanamori's (GK) rules, many ferromagnets have been designed through the coupling of two B site ions with and without  $e_g$  electrons. In BFM, the 180 degree  $-\text{Fe}^{3+}\text{-O-Mn}^{3+}$  bonds is quasistatic, partly because the strong Jahn-Teller uniaxial strain in an octahedral site. Because the complication of the double perovskite system, there are still some questions about the violation of GK rules in some cases and the origin of the ferromagnetism or antiferromagnetism. The other problem is the bad ferroelectric properties. In order to characterization of their ferroelectric/piezoelectric properties, scanning probe microscopy (SPM) techniques were used.

Multiferroic materials can be classified into two categories: one is single-phase materials; the other is multilayer or composite hetero-structures that contain more than one ferroic phases [5]. The most desirable multiferroic material is the intrinsic single-phase material, which is

still rarely produced although significant advancements had been made recently. Therefore, it is essential to broaden the searching field for new candidates of multiferroics. This work focuses on both types multiferroic materials: Single-phase  $\text{Bi}_2\text{FeMnO}_6$  and multilayered  $\text{YMnO}_3/\text{SnTiO}_3$ . Scanning probe microscopy (SPM) techniques were used for ferroelectric domain imaging of these multiferroic materials.

As we know, most piezoelectric/ferroelectric materials with good performances are based on the perovskite-type oxides of  $\text{ABO}_3$ , among them, the most extensively studied ones should be  $\text{PbTiO}_3$  and  $\text{Pb}(\text{ZrTi})\text{O}_3$  based materials due to their high dielectric constants and good piezoelectric/ferroelectric properties. However, these materials containing lead which leads to environmental problems. Thus, it is desirable to develop new lead-free piezoelectric materials to replace PZT based piezoelectrics for environmental protection. Through first principle calculations,  $\text{SnTiO}_3$  containing  $\text{Sn}^{2+}$  ions was estimated to have excellent ferroelectric properties [6, 7]. The calculated results indicated that the spontaneous polarization and piezoelectric coefficients of  $\text{SnTiO}_3$  is comparable with those of  $\text{PbTiO}_3$ . Moreover, the most stable structure is tetragonal perovskite with  $a=b=3.80\text{\AA}$  and  $c=4.09\text{\AA}$  [6, 7]. The metastable  $\text{SnTiO}_3$  phase is very difficult to obtain, a good way to stabilize the  $\text{SnTiO}_3$  phase is to mix it with other compounds. Several studies have been focused on the synthesis of Sn-doped ceramics in  $\text{BaTiO}_3$  system, such as  $(\text{Ba}_{0.6}\text{Sr}_{0.4})(\text{Ti}_{1-x}\text{Sn}_x)\text{O}_3$  [8],  $(\text{Ba}_{1-x-y}\text{Ca}_x\text{Sn}_y)\text{TiO}_3$  [9]. However, it is difficult to obtain  $\text{Sn}^{2+}$  by traditional bulk synthesis techniques. On the other hand, it is easier to fabricate  $\text{SnTiO}_3$  using pulsed laser deposition method (PLD). Our interest was to find out whether the  $\text{SnTiO}_3$  phase can be stabilized through the layer-by-layer deposition using PLD, and whether it is possible to obtain such metastable materials in non-equilibrium conditions.

The hexagonal manganite  $\text{YMnO}_3$ , which shows an antiferromagnetic transition at  $T_N = 75\text{ K}$ , and a ferroelectric transition  $T_C = 913\text{ K}$ , is one of the rare existing multiferroics [10-12]. It was chosen as the basic composition to sandwich  $\text{SnTiO}_{3+x}$  phase and to form YST multilayer film. In this work, we reported the effect of substrate orientation and layer numbers of  $\text{YMnO}_3$  and  $\text{SnTiO}_{3+x}$  on the piezoelectric/ferroelectric and magnetic properties in the designed layered YST system. It was hoped that our method would serve as a model system to introduce the use of PLD techniques in the growth of multilayer multiferroic materials and metastable materials. Such techniques could be promising for device design and the searching in fabricating new materials.

## 2. SPM system

SPM has emerged as a powerful tool for high-resolution characterization of ferroelectrics for the first time providing an opportunity for non-destructive visualization of ferroelectric domain structures at the nanoscale. [13] These nanostructures can be used for studying the intrinsic size effects in ferroelectrics as well as for addressing such technologically important issues as processing damage, interfacial strain, grain size, aspect ratio effect, edge effect, domain pinning and imprint. [14] The system composes of a conducting tip in con-

tact with the dielectric surface on a conductive substrate can be considered as a capacitor. SPM is a well-established field offering multiple opportunities for new discoveries and breakthroughs. [15-17]

Piezoelectric materials provide an additional response to the applied ac electric field due to the converse piezoelectric effect:  $\Delta l = d_{33} V$ , where  $\Delta l$  is the displacement,  $d_{33}$  is the effective longitudinal piezoelectric coefficient. [18, 19] It follows that both electrostatic and piezoelectric signals are linear with the applied voltage and thus contribute to the measured PFM response. These measurements are referred to as out-of-plane (OP) measurement. Measurements of local hysteresis loops are of great importance in inhomogeneous or polycrystalline ferroelectrics because they are able to quantify polarization switching on a scale significantly smaller than the grain size or inhomogeneity variation. Macroscopically, the switching occurs via the nucleation and growth of a large number of reverse domains in the situation where the applied electric field is uniform. Therefore, the  $d_{33}$  hysteresis reflects the switching averaged over the entire sample under the electrode. [20, 21] In the PFM experimental conditions, the electric field is strongly localized and inhomogeneous; therefore, the polarization switching starts with the nucleation of a single domain just under the tip.

### 3. Material designation and characterization

Multiferroic materials have been attracting considerable attention especially in the last ten years. [22-25] One of the most appealing aspects of multiferroics is their magnetoelectric coupling. Among them, the most studied is the perovskite  $\text{BiFeO}_3$  (BFO) with room temperature multiferroic properties and  $\text{YMnO}_3$ . Based on BFO and  $\text{YMnO}_3$ , we designed new multiferroics and fabricated the films using pulsed laser deposition (PLD) method. The material system includes double perovskite multiferroic  $\text{Bi}_2\text{FeMnO}_6$  (BFM) and multilayered  $\text{YMnO}_3/\text{SnTiO}_{3+x}$  (YST). Compared to BFO, the magnetic properties of BFM and YST were greatly improved. However, until now there is no report about their ferroelectric properties because the difficulty of obtaining well-shaped polarization hysteresis loops. It is important to study ferroelectric properties because the possible coupling between ferroelectric and antiferromagnetic domains and its lead-free nature. As is well known, the ferroelectric property is mainly determined by the domain structures and domain wall motions. The most exciting recent developments in the field of multiferroics and the most promise for future discoveries are in interfacial phenomena. [26] The interfaces include those that emerge spontaneously and those that are artificially engineered. Therefore, the domain structure and polarization switching were studied in these three new multiferroic films using piezoresponse force microscopy (PFM).

The emerging technique of PFM is proved to be a powerful tool to study piezoelectric and ferroelectric materials in such cases and extensive contributions have been published. In PFM, the tip contacts with the sample surface and the deformation (expansion or contraction of the sample) is detected as a tip deflection. The local piezoresponse hysteresis loop and information on local ferroelectric behavior can be obtained because the strong coupling

between polarization and electromechanical response in ferroelectric materials. In the present study, we attempt to use PFM to study the ferroelectric/piezoelectric properties in films of BFM and YST. PFM response was measured with a conducting tip (Rh-coated Si cantilever,  $k \sim 1.6 \text{ N m}^{-1}$ ) by an SII Nanotechnology E-sweep AFM. PFM responses were measured as a function of applied DC bias ( $V_{dc}$ ) with a small ac voltage applied to the bottom electrode (substrate) in the contact mode, and the resulting piezoelectric deformations transmitted to the cantilever were detected from the global deflection signal using a lock-in amplifier.

### 3.1. Characterization of BFM film

Magnetism and ferroelectricity exclude each other in single phase multiferroics. It is difficult for designing multiferroics with good magnetic and ferroelectric properties. Our interest is to design new candidate multiferroics based on  $\text{BiFeO}_3$ .  $\text{BiFeO}_3$  is a well-known multiferroic material with antiferromagnetic Neel temperature of 643K, which can be synthesized in a moderate condition. [22, 23, 25] In contrast,  $\text{BiMnO}_3$  is ferromagnetic with  $T_c = 110\text{K}$  and it needs high-pressure synthesis. [27, 28] The possible magnetoelectric coupling has motivated a lot of studies on the ferroelectric and antiferromagnetic domains. The ferroelectric domain structures of BFO in the form of ceramics, single crystals and thin films have been intensively studied using PFM, TEM and other techniques.

Single phase BFM ceramics could be synthesized by conventional solid state method as the target. For BFM ceramics, the starting materials of  $\text{Bi}_2\text{O}_3$ ,  $\text{Fe}_3\text{O}_4$ ,  $\text{MnCO}_3$  were weighed according to the molecular mole ratio with 10 mol% extra  $\text{Bi}_2\text{O}_3$ . They were mixed, pressed into pellets and sintered at  $800^\circ\text{C}$  for 3 h. Then the ceramics were crushed, ground, pressed into pellets and sintered again at  $880^\circ\text{C}$  for 1 h. BFM films were deposited on  $\text{SrTiO}_3$  (STO) substrate by pulsed laser deposition (PLD) method at  $650^\circ\text{C}$  with 500 ~ 600mTorr dynamic oxygen. [29, 30]

The structure of BFM was calculated [31] and it is connected with the magnetic configurations as shown in Figure 1. It has three possible space groups of  $\text{Pm}\bar{3}\text{m}$ ,  $\text{R}\bar{3}$  and  $\text{C}2$  and the magnetic configurations were presumed for each structure symmetry to be G-type antiferromagnetic (G-AFM) and ferromagnetic (FM) structures. The most stable structure of BFM is monoclinic with  $\text{C}2$  space group. Mn tends to show 3+ valence which will induce a large distortion because it is Jahn-Teller ion. The valence of Mn and Fe has been studied in the former work. [30, 32]

Figure 2 shows the results of the PFM images of BFM film. Several features could be observed: firstly, the obvious contrast could be seen and the grains in PFM and topography are correspondence; secondly, the existence of contrasts on both OP and IP indicates multiple orientations of domains; thirdly, the IP contrast is not so clear as OP contrast, that is to say, the suppression of the in-plane response for heterostructures suggesting a constrained ferroelectric domain-orientation along the OP direction. In the former paper, the ferroelectric domain switching and typical butterfly loops were observed. [32]



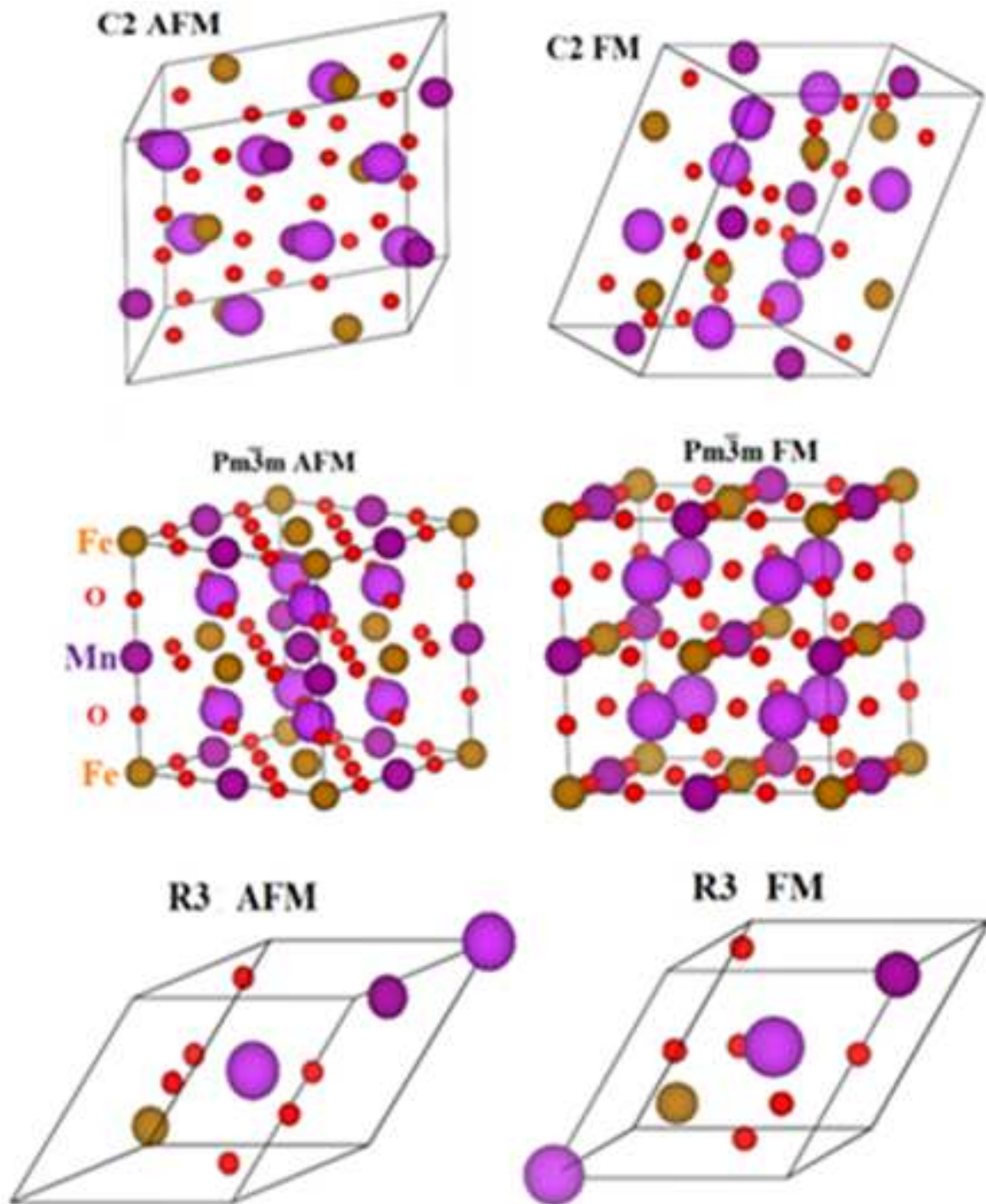


**Figure 1.** Calculated six structures of BFM.

The domains in BFO films have been analyzed in detail in Ref [19]: the bigger spontaneous ferroelectric domains were observed in BFO than in other ferroelectrics without multiferroic properties; the domains were irregular but the the model was predicted and consistent with the experimental results. According to the present results of BFM, further study is needed to obtain the domain morphology and do the calculation.

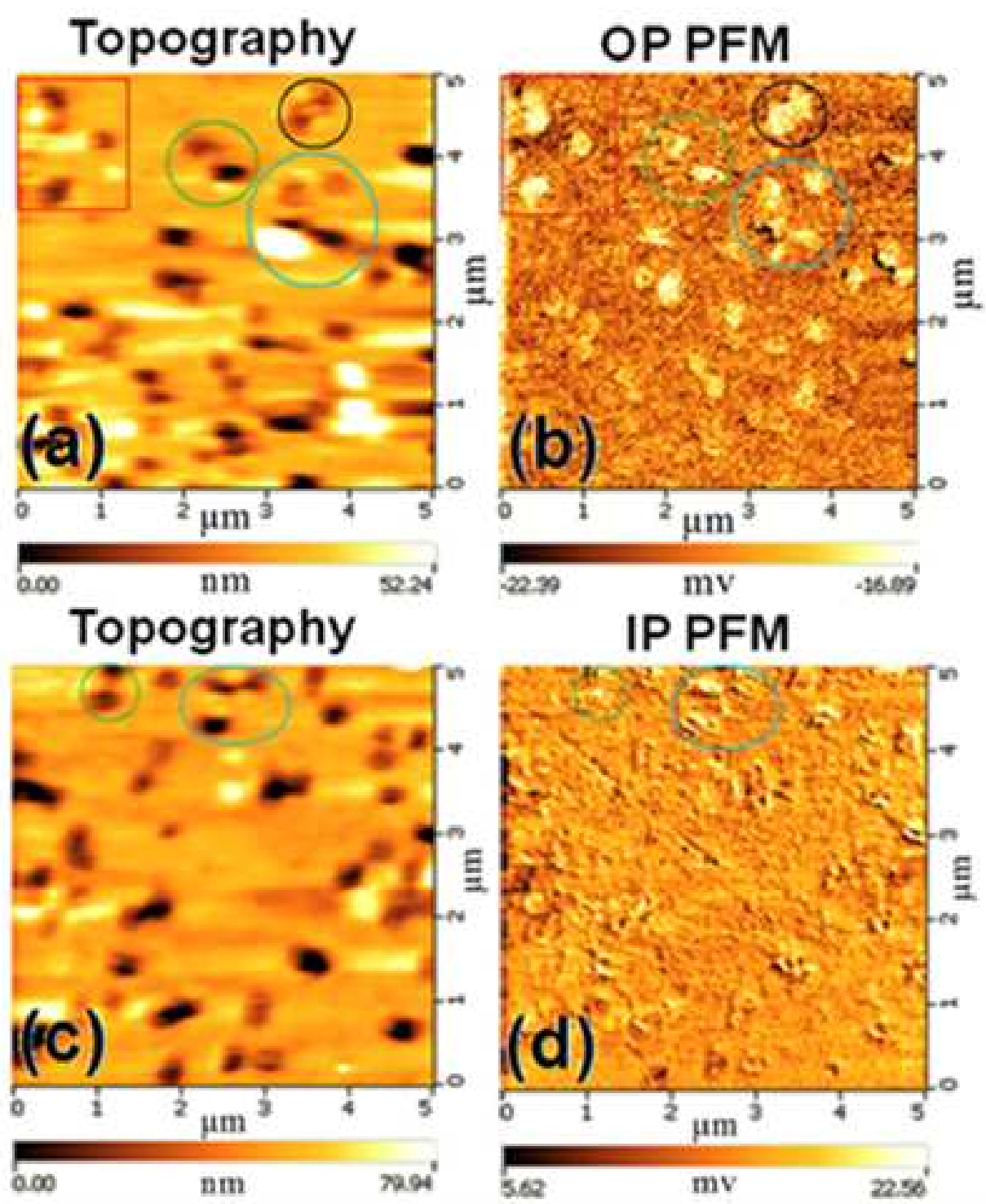


Figure 2. PFM images of BFM film

### 3.2. Characterization of YST film

Polycrystalline  $\text{YMnO}_3$  and  $\text{TiO}_2$  ceramics were synthesized by conventional solid state method as the targets. On addition the  $\text{SnO}$  and  $\text{SnO}_2$  commercial targets were also used at the same time in our process. The deposition of these films includes the following major steps. YST films were deposited on (100) and (110) Nb:  $\text{SrTiO}_3$  (STO) substrate using a pulsed laser deposition (PLD) system at  $700^\circ\text{C}$  with  $10^{-1} \sim 10^{-5}$  Torr dynamic oxygen. The targets were alternately switched constantly and the films were obtained in a layer-by-layer growth mode. After deposition, the films were annealed in the same condition for 15 minutes at  $700^\circ\text{C}$  and then cooled to room temperature. [33]

In YST multilayered films, one layer is defined to be comprised of two sub-layers: (1)  $\text{YMnO}_3$  and (2)  $\text{SnTiO}_{3+x}$ . The films deposited on (100), (111) and (110) STO are expressed as YST100, YST111 and YST110, respectively. The film YST110-4 denotes the films deposited on (110) STO with four layers, as shown clearly in Figure 3. The total deposition time for  $\text{YMnO}_3$  and  $\text{SnTiO}_{3+x}$  is the same of 40 and 20 minutes, respectively.

XRD patterns for the five films of YST100-2, YST100-4 were shown in Figure 4. The peaks were identified using the XRD results of  $\text{SnTiO}_3$  ( $\odot$ ),  $\text{YMnO}_3$  ( $\text{Y}$ ) (shown in Figure 9,  $\text{FeTiO}_3$  ( $\nabla$ ) [34, 35].  $\text{SnTiO}_3$  is metastable and it showed two combined phases, one is  $\text{FeTiO}_3$ , and the other is the good ferroelectric phase which has tetragonal structure. XRD patterns of  $\text{SnTiO}_3$  ( $\odot$ ) were shown in Figure 5 in supplementary materials, which is obtained using the calculated data[6, 7]. The symbol of “?” represents the phase which we cannot identify so far, it could be a peak from the (111)  $\text{TiO}_2$  phase.

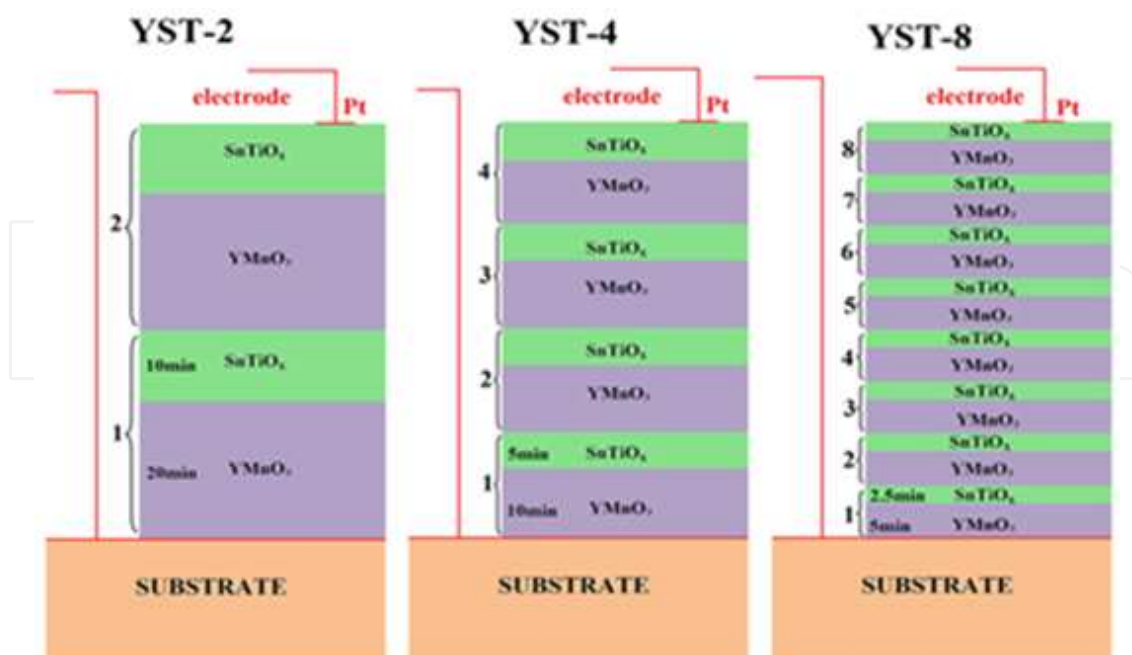


**Figure 3.** Schematic explanation of films with two, four and eight layers, each layer contains two sublayers of  $\text{YMnO}_3$  and  $\text{SnTiO}_3$ .



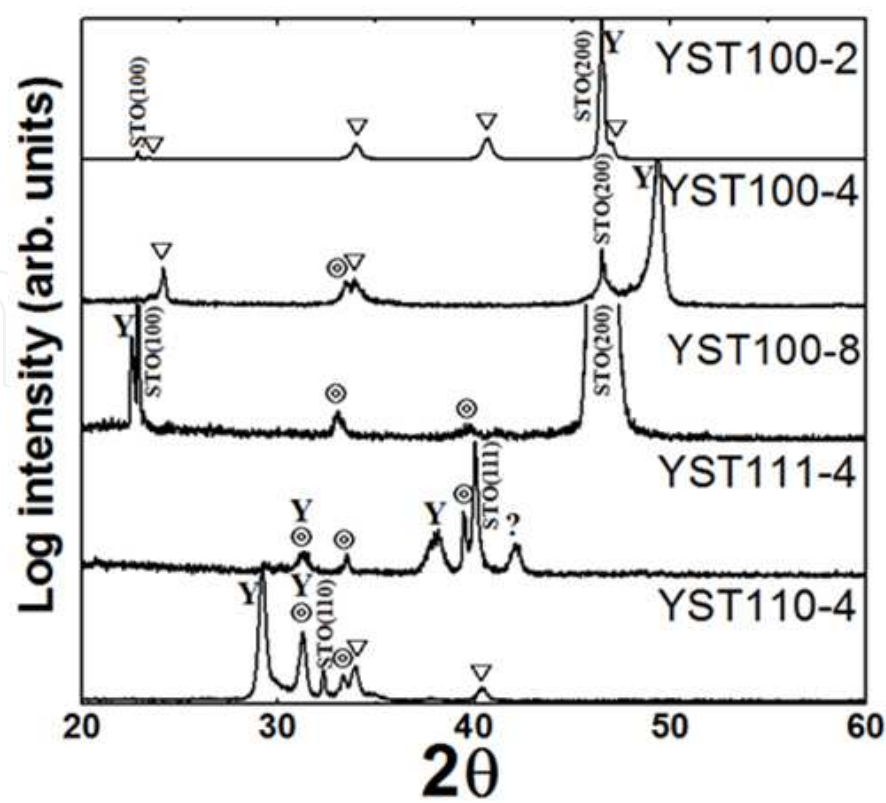


Figure 4. XRD patterns for the five films of YST100-2, YST100-4. [31]

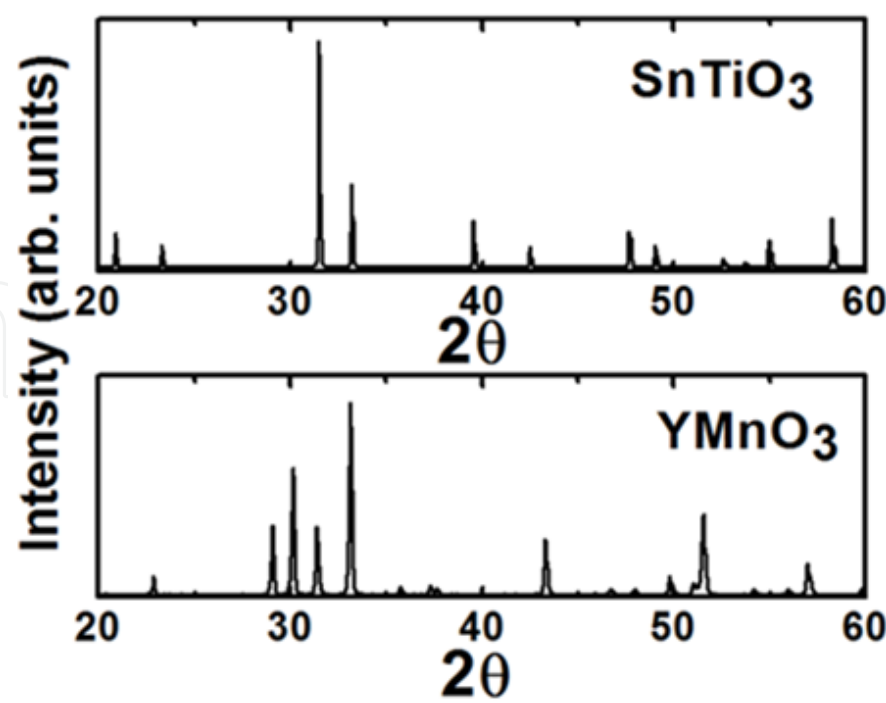
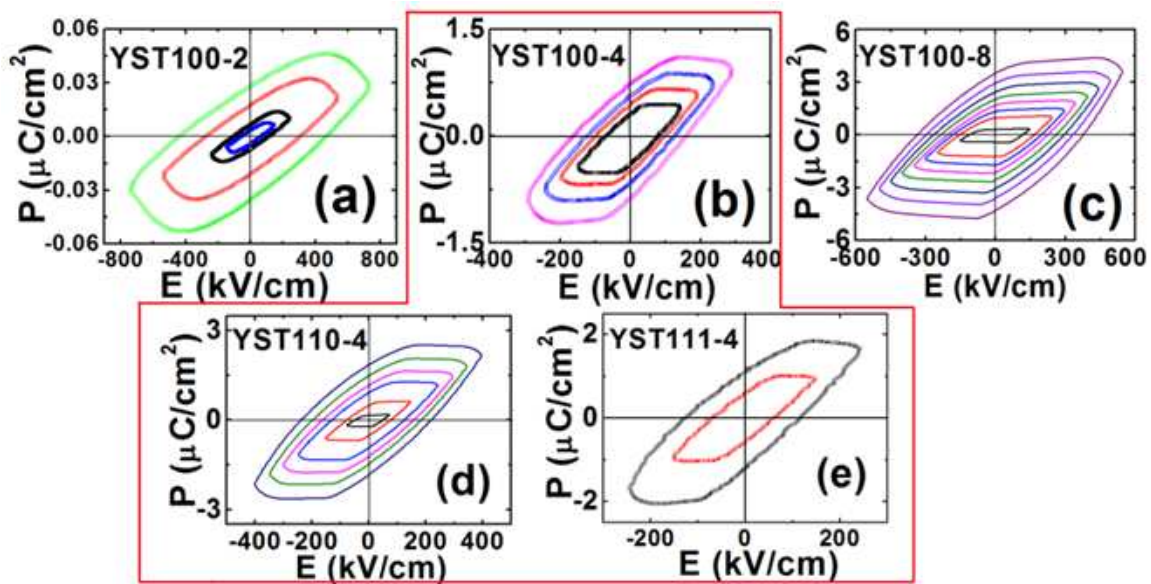


Figure 5. XRD patterns of calculated  $\text{SnTiO}_3$  and  $\text{YMnO}_3$  targets. [33]

Many reports about the  $\text{YMnO}_3$  films can be found but most of them without ferroelectric characterization provided. This is mainly ascribed to the difficulty in obtaining a satisfactory ferroelectric measurement result. Figure 6 shows the electrical polarization hysteresis loops (P-E loops) of YST110-4 film. The ferroelectric type hysteresis loop was observed. It is obvious that the P-E loop is significantly different for different layer-number films, as well as for different substrate orientations. For the same STO orientation, the P-E loops were improved as the layer number increase, and the film fabricated on (110) STO shows improved properties compared to the film on (100) STO with the same layer number. As for the same deposition time for the four samples, it is found that more layers of  $\text{SnTiO}_3$  in the YST system shows much better ferroelectric properties. It is suggested that the  $\text{SnTiO}_3$  phase can exist only in ultra-thin thickness and can be stabilized by  $\text{YMnO}_3$  sub-layers. That is to say,  $\text{SnTiO}_3$  is indeed a ferroelectric materials but it is a great challenge [36] to obtain stable single phase  $\text{SnTiO}_3$  films that is with good ferroelectric performance (it will be tried in our future works). Although the electric charge in the interface may affect its ferroelectric properties, the improved properties of YST110-4 proved that its effect was not significant. While the P-E loops were not improved in YST111-4, all the observations showed the anisotropy of the films.



**Figure 6.** Ferroelectric polarization loop of YST films. [31]

Although well developed P-E loops were observed for YST100-8 and YST110-4, the loops still show the rounded features, indicating that contributions to the hysteresis loop from movable charges was significant. In addition, the P-E loops of the four films have revealed that the polarization is rather small (just a few  $\mu\text{C}/\text{cm}^2$ ) and they do not exhibit saturation. The fatigue properties were shown in Figure 7 for YST110-4. The polarization measurement was at 21V, the switching voltage was 14V and the frequency was 5k Hz. The remnant polarization decreased about 40% after  $10^7$  read/write cycles for YST110-4. From all the comparisons, YST110-4 sample shows the comparable ferroelectric properties with YST100-8.

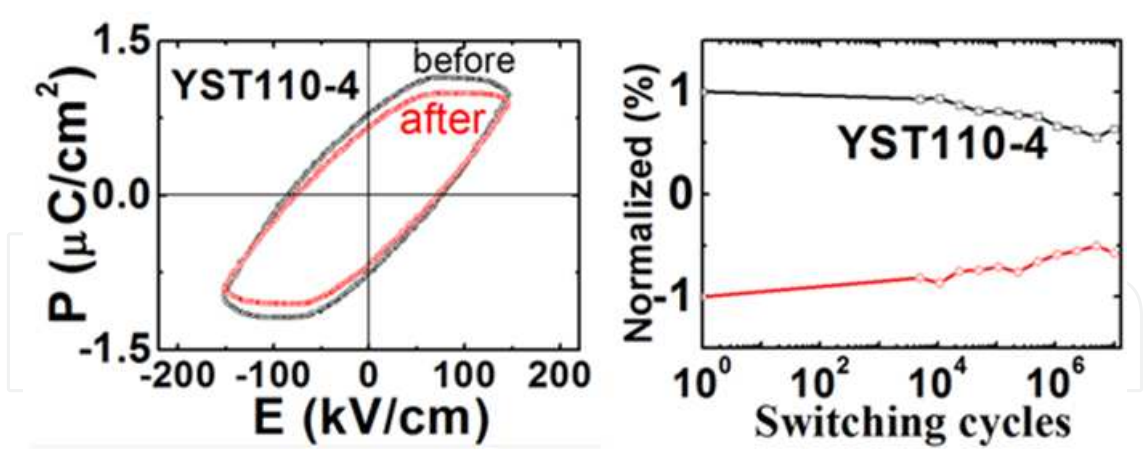


**Figure 7.** Fatigue measurement of YST110-4 film. [31]

Figure 8 shows TEM results of the YST110-4 film. It clearly shows four layers and one layer which is close to the substrate seems have some reaction with the substrate. The other three layers are homogeneous and we could see the domain structures through this image. The surface of the film was studied using AFM as shown in Figure 9. As expected, Figure 10 displays contrast over the polarized square after poled by positive and negative 10 V voltage, due to the different phases of the PFM response for the up and down domains. The obvious change of the contrast in YST110-4 film confirms that the polarization reversal is indeed possible and that the film is ferroelectric at room temperature.

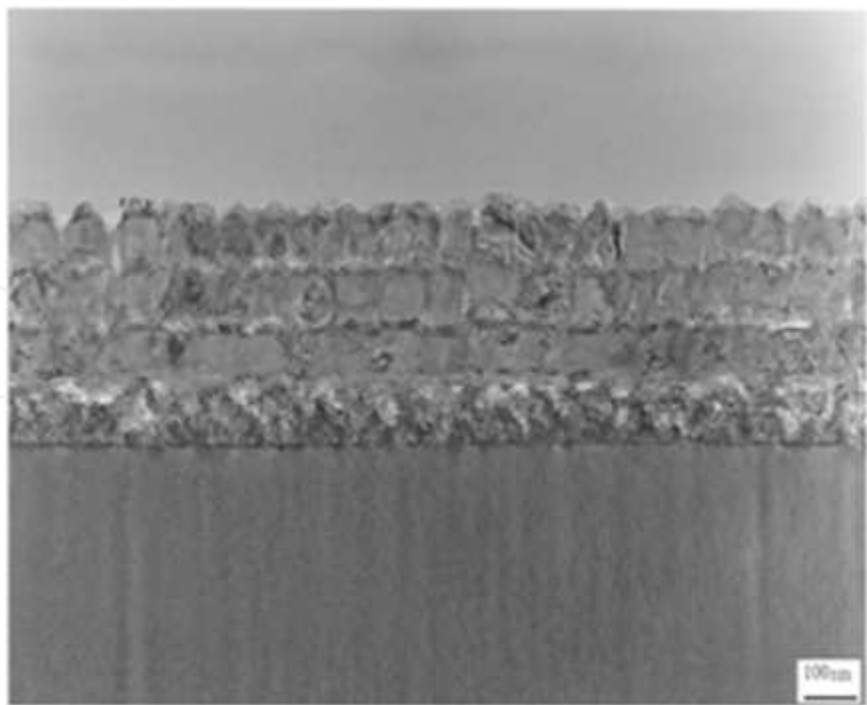


**Figure 8.** TEM image of YST110-4 film.

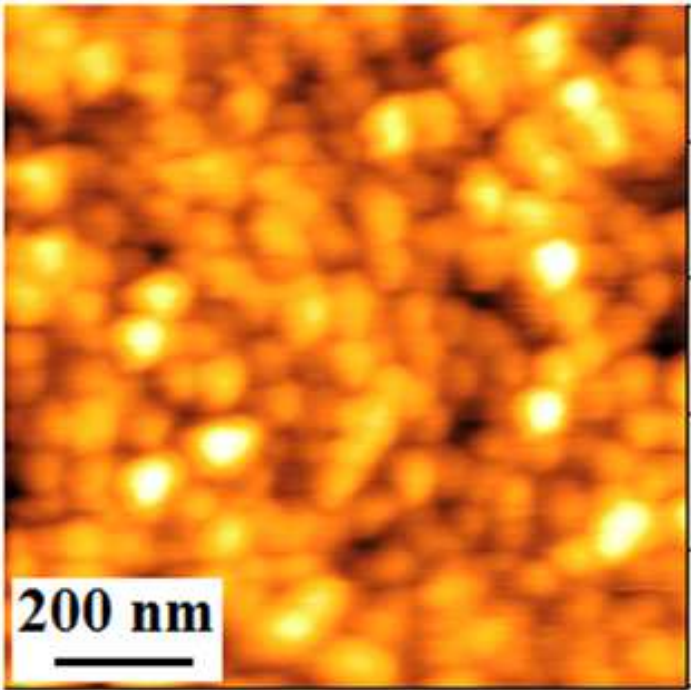


**Figure 9.** AFM topography image of YST110-4 film.

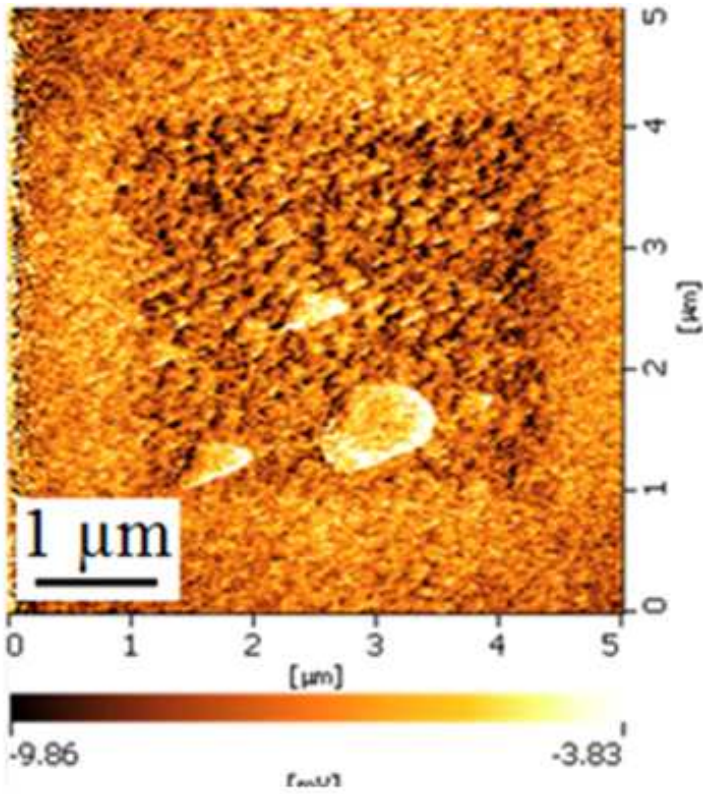


**Figure 10.** PFM image of YST110-4 film after poled using  $\pm 10$  V voltage



As seen in Figure 11, when a direct current voltage up to 10 V was applied on the samples, the sample exhibited “butterfly” loop. The loops were not symmetrical due to the asymmetry of the upper (tip) and bottom (substrate) electrodes. In addition, the substrate may also affect the  $d_{33}$ . According to the equation  $d_{33} = \Delta l / V$ , where  $\Delta l$  is the displacement, the effective  $d_{33}$  could be calculated. At the voltage of 10 V, both samples show the maximum effective  $d_{33}$  of about 6.21 pm/V for YST110-4 sample.

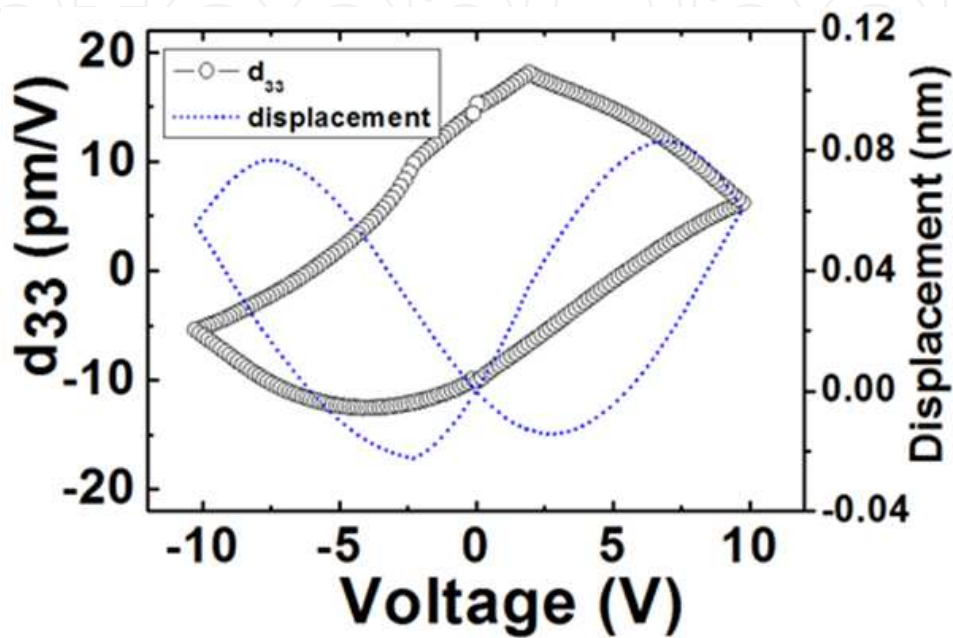


**Figure 11.** Butterfly and local piezoresponse hysteresis loops of YST110-4 film.

#### 4. Conclusions

The novel multiferroic films of BFM and multilayered YST were successfully produced using PLD method. Both of them were characterized using PFM method. The special or excellent properties can often be found in the metastable materials. Through calculation, six structures are presumed in BFM with two magnetic configurations of G-AFM and FM. In YST films, the metastable  $\text{SnTiO}_3$  phase was obtained. The improved ferroelectric properties were observed through increasing the layer numbers and more  $\text{SnTiO}_3$  phase was stabilized, moreover, the change in contrast after bias is applied indicates a change in polarization direction and hence ferroelectric switching. Although it is a great challenge in obtaining the  $\text{SnTiO}_3$  thin films, we believe that through the optimization of fabrication process and conditions, the single phase  $\text{SnTiO}_3$  or multilayer films, or composite materials containing  $\text{SnTiO}_3$  could become a new generation lead-free piezoelectric/ferroelectric material. For a thorough understanding of the mechanisms of the films, knowledge of the domain structures is a prerequisite, which is of crucial importance to increase and tune the functionality of multiferroic films.



## Acknowledgements

The authors gratefully acknowledge Dr. Minoru Osada, Dr. Kazuya Terabe in NIMS and Prof. H. R. Zeng in Shanghai Institute of Ceramics for their experimental help and discussions. Part of this work was supported by JST ALCA and MEXT GRENE.

## Author details

Hongyang Zhao<sup>1,2\*</sup>, Hideo Kimura<sup>1</sup>, Qiwen Yao<sup>1</sup>, Lei Guo<sup>1</sup>, Zhenxiang Cheng<sup>3</sup> and Xiaolin Wang<sup>3</sup>

\*Address all correspondence to: [zhao.hongyang@nims.go.jp](mailto:zhao.hongyang@nims.go.jp)

1 National Institute for Materials Science, Sengen 1-2-1, Tsukuba, Japan

2 Shanghai Institute of Ceramics, Chinese Academy of Sciences, Shanghai, China

3 Institute for Superconducting and Electronics Materials, University of Wollongong, Innovation Campus, Fairy Meadow, Australia

## References

- [1] Hill N. A., Why are there so few magnetic ferroelectrics? J. Phys. Chem. B 2000; 104: 6694.
- [2] Fiebig M., T. Lottermoser, D. Frohlich, A. V. Goltsev, R. V. Pisarev, Observation of coupled magnetic and electric domains. Nature 2002; 419: 818.
- [3] Eerenstein W., Mathur N. D. and Scott J.F., Multiferroic and magnetoelectric materials. Nature 2006; 442: 759-765.
- [4] Singh M. K., Prellier W., Singh M. P., Katiyar R. S., Scott J. F., Spin-glass transition in single-crystal BiFeO<sub>3</sub>. Phys. Rev. B 2008; 77: 144403.
- [5] J. Das, Y.Y. Song, M.Z. Wu, Electric-field control of ferromagnetic resonance in monolithic BaFe<sub>12</sub>O<sub>19</sub>-Ba<sub>0.5</sub>Sr<sub>0.5</sub>TiO<sub>3</sub> heterostructures. J. Appl. Phys. 2010; 108: 043911.
- [6] Konishi Y., Ohasawa M., Yonezawa Y., Tanimura Y., Chikyow T., Wakisaka T., Koinuma H., Miyamoto A., Kubo M., Sasata K., Mater. Res. Soc. Symp. Proc. 2003; 748 U3.13.1.
- [7] Uratani Y., Shishidou T., Oguchi T., First-Principles Study of Lead-Free Piezoelectric SnTiO<sub>3</sub>. Jpn. J. Appl. Phys. 2008; 47 (9), 7735-7739.

- [8] Ha J. Y., Lin L. W., Jeong D. Y., Yoon S. J., Choi J. W., Improved Figure of Merit of (Ba,Sr)TiO<sub>3</sub>-Based Ceramics by Sn Substitution. Jpn. J. Appl. Phys. 2009; 48 011402.
- [9] Suzuki S., Takeda T., Ando A., Takagi H., Ferroelectric phase transition in Sn<sup>2+</sup> ions doped (Ba,Ca)TiO<sub>3</sub> ceramics. Appl. Phys. Lett. 2010; 96: 132903.
- [10] Marin L.W., Crane S.P., Chu Y-H., Holcomb M.B., Gajek M., Huijben M., Yang C-H., Balke N., Ramesh R., Multiferroics and magnetoelectrics: thin films and nanostructures. J. Phys.: Condens. Matter 2008; 20: 434220.
- [11] Yakel H.L., Koehler W.C., Bertaut E.F., Forrat E.F., On the crystal structure of the manganese(III) trioxides of the heavy lanthanides and yttrium. Acta Crystallogr. 1963; 16: 957-962.
- [12] Bertaut E. F., Pauthenet R., Mercier M., Proprietes magnetiques et structures du manganite d'yttrium. Phys. Lett. 1963; 7: 110-111.
- [13] Gruverman A, Kholkin A, Nanoscale Ferroelectrics: Processing, Characterization and Future Trends. Rep. Prog. Phys. 2006; 69: 2443-2474.
- [14] Catalan G., Noheda B, McAneney J, Sinnamon L J, Gregg J M Strain gradients in epitaxial ferroelectrics. Phys. Rev. B 2005; 72: 0201102.
- [15] Muralt P. J. Micromech. Ferroelectric thin films for micro-sensors and actuators. Microeng. 2000; 10: 136.
- [16] Terabe K, Nakamura M, Takekawa S, Kitamura K, Higuchi S, Gotoh Y, Cho Y Microscale to nanoscale ferroelectric domain and surface engineering of a near-stoichiometric LiNbO<sub>3</sub> crystal. Appl. Phys. Lett. 2003; 82: 433-435.
- [17] Fong D D, Stephenson G B, Streigger S K, Eastman J A, Auciello O, Fuoss P H, Thompson C Ferroelectricity in ultrathin perovskite films Science. 2004; 304: 1650.
- [18] Kholkin A L, Bdikin I K, Shvartsman V V, Orlova A, Kiselev D, Bogomolov V, MRS Proc. E 2005; 838: O7.6.
- [19] Catalan G., Bea H., Fusil S., Bibes M., Paruch P., Barthelémy A., Scott J. F., Fractal Dimension and Size Scaling of Domains in Thin Films of Multiferroic BiFeO<sub>3</sub>. Phys. Rev. Lett. 2008; 100 027602.
- [20] Kalinin S V, Gruverman A and Bonnell D A Quantitative analysis of nanoscale switching in SrBi<sub>2</sub>Ta<sub>2</sub>O<sub>9</sub> thin films by piezoresponse force microscopy Appl. Phys. Lett. 2004; 85: 795-797
- [21] Tybell T, Paruch P, Giamarchi T, Triscone J-M Domain wall creep in epitaxial ferroelectric Pb(Zr<sub>0.2</sub>Ti<sub>0.8</sub>)O<sub>3</sub> thin films 2002 Phys. Rev. Lett. 89 097601
- [22] Catalan G., Scott J. F., Adv. Mater. Physics and Applications of Bismuth Ferrite. 2009; 21, 2643.
- [23] Wang J., Neaton B. J., Zheng H., Nagarajan V., Ogale S. B., Liu B., Viehland D., Vaitheyanathan V., Schlom D. G., Waghmare U. V, Spaldin N. A., Rabe K. M., Wutting

- M., Ramesh R., Epitaxial BiFeO<sub>3</sub> Multiferroic Thin Film Heterostructures. *Science* 2003; 299: 1719-1722.
- [24] Kimura T., Goto T., Shintani H., Ishizaka K., Arima T., Tokura Y., Magnetic Control of Ferroelectric Polarization. *Nature* 2003; 55: 426.
- [25] Cheng Z. X., Wang X. L., Dou S. X., Ozawa K., Kimura H., Improved ferroelectric properties in multiferroic BiFeO<sub>3</sub> thin films through La and Nb codoping. *Phys. Rev. B* 2008; 77: 092101.
- [26] Spaldin N. A., Cheong S. W., Ramesh R., Multiferroics: Past, present, and future. *Physics Today* 2010; 63: 38-43.
- [27] T. Atou, H. Chiba, K. Ohoyama, Y. Yamaguchi, Y. Syono, Structure determination of ferromagnetic perovskite BiMnO<sub>3</sub>. *J. Solid State Chem.* 1999; 145(2) 639-642.
- [28] T. Kimura, S. Kawamoto, I. Yamada, M. Azuma, M. Takano, Y. Tokura, Magnetocapacitance effect in multiferroic BiMnO<sub>3</sub>, *Phys. Rev. B* 2003; 67 (R), 180401-180404.
- [29] Zhao, H.Y.; Kimura, H.; Cheng, Z.X.; Wang, X.L. & Nishida, T. Room temperature multiferroic properties of Nd:BiFeO<sub>3</sub>/Bi<sub>2</sub>FeMnO<sub>6</sub> bilayered films. *Appl. Phys. Lett.* 2009; 95(23)232904
- [30] Zhao, H.Y.; Kimura, H.; Cheng, Z.X.; Wang, X.L.; Ozawa, K. & Nishida, T. Magnetic characterization of Bi<sub>2</sub>FeMnO<sub>6</sub> film grown on (100) SrTiO<sub>3</sub> substrate *Phys. Status Solidi RRL* 2010; 4(11) 314.
- [31] Bi, L.; Taussig, A.R.; Kim, H-S.; Wang, L.; Dionne, G.F.; Bono, D.; Persson, K.; Ceder, G. & Ross, C.A. Structural, magnetic, and optical properties of BiFeO<sub>3</sub> and Bi<sub>2</sub>FeMnO<sub>6</sub> epitaxial thin films: An experimental and first-principles study. *Phys. Rev. B* 2008; 78 (10) 104106.
- [32] Zhao H Y, Kimura H.; Cheng Z.X.; Wang X.L., New multiferroic materials: Bi<sub>2</sub>FeMnO<sub>6</sub>. *Ferroelectrics-Material Aspects. InTech*; 2011.
- [33] Zhao H Y, Kimura H.; Cheng Z.X.; Wang X.L., Yao Q W, Osada M, Li B W, Nishida T A new multiferroic heterostructure of YMnO<sub>3</sub>/SnTiO<sub>3</sub>+x. *Scrip. Mater.* 2011; 65: 618-621
- [34] Harrison R.J., Redfern S.A.T., Smith R.I., Thermodynamics of the R $\bar{3}$  to R $\bar{3}$  phase transition in the ilmenite-hematite solid solution. *Am. Mineral.* 2000; 85: 1694-1705.
- [35] Leinenweber K., Utsmi W., Tsuchida Y., Yagi T., Kuita K., Unquenchable High-Pressure Perovskite Polymorphs Of MnSnO<sub>3</sub> And FeTiO<sub>3</sub>. *Phys. Chem. Miner.* 1991; 18: 244.
- [36] Venkatesan S., Daumont C., Kooi B.J., Noheda B., J Hossoneff Th.M. De, Nanoscale domain evolution in thin films of multiferroic TbMnO<sub>3</sub>. *Phys. Rev. B* 2009; 80: 214111.

